# Time-dependent material properties and reinforced beams behavior of two alkali-activated types of concrete

Prinsse, Silke; Hordijk, Dick A.; Ye, Guang; Lagendijk, Paul; Luković, Mladena

**DOI**
10.1002/suco.201900235

**Publication date**
2019

**Document Version**
Final published version

**Published in**
Structural Concrete

**Citation (APA)**
Prinsse, S., Hordijk, D. A., Ye, G., Lagendijk, P., & Luković, M. (2019). Time-dependent material properties and reinforced beams behavior of two alkali-activated types of concrete. *Structural Concrete*, *21 (2020)*(2), 642-658. https://doi.org/10.1002/suco.201900235

Received: 18 June 2019 | Revised: 15 August 2019 | Accepted: 20 September 2019

DOI: 10.1002/suco.201900235

TECHNICAL PAPER

fib CEB-FIP WILEY

# Time-dependent material properties and reinforced beams behavior of two alkali-activated types of concrete

**Silke Prinsse | Dick A. Hordijk | Guang Ye | Paul Lagendijk | Mladena Luković**

Delft University of Technology, Delft, the Netherlands

**Correspondence**
Mladena Luković, Delft University of Technology, Stevinweg 1, 2628 CN Delft, the Netherlands.
Email: m.lukovic@tudelft.nl

**Funding information**
4TU.Bouw Lighthouse project "Towards a Geopolymer Concrete Bridge"

## Abstract

This paper presents an experimental study on the development of material properties over time (up to around 2 years) and the structural behavior of reinforced beams, for two types of alkali-activated concrete (AAC). Compressive strength, flexural strength, tensile splitting strength, elastic modulus, and flexural behavior of reinforced beams are investigated. Tested material properties of AAC are compared with the properties of conventional concrete, as predicted by Eurocode. For the mixes of AAC and the conventional concretes with the same 28 days compressive strength, flexural and tensile splitting strength at 28 days are found to be similar, whereas the elastic moduli of AAC mixtures is up to 30% lower than those of conventional concrete. Related to the long term behavior, after 28 days moist-curing and subsequently exposing AAC specimens to laboratory conditions (50% RH/20°C), a reduction of flexural strength, tensile splitting strength and elastic modulus, is observed. Structural behavior of the reinforced AAC beams in four-point bending test seems not to be affected significantly by the observed decrease in material properties, and is found to be similar to that of conventional concrete beams. The acquired results indicate that the observed decrease of material properties over time might be related to drying (moisture loss). However, more research is needed to understand the phenomenon, especially related to the aimed structural application and safe upscaling of AAC.

**KEYWORDS**

alkali-activated concrete, alkali-activated slag, reinforced alkali-activated concrete beams, stiffness, strength, structural behavior, time-dependent behavior

## 1 | INTRODUCTION

During the last century, concrete has become the most popular construction material. Mostly due to its ease of use, overall availability, freedom of form, and good performance, concrete is, next to water, the mostly consumed substance on earth.[1] In order to make concrete, a binder is needed for which the combination of Ordinary Portland Cement (OPC) and water is conventionally used. The widespread availability and relatively low costs of the needed materials and technologies to produce OPC, contributed to the fact that it became the highest-volume manufactured product on the planet.[2] However, the production of OPC is energy-intensive and the ever-growing cement production also implies overexploitation of natural resources such as

Discussion on this paper must be submitted within two months of the print publication. The discussion will then be published in print, along with the authors' closure, if any, approximately nine months after the print publication.

limestone quarries.[3] Moreover, cement production is one of the primary contributors to global warming, accounting for at least 5–8% of worldwide anthropogenic $CO_2$ emissions.[4]

The environmental impact of concrete production can be reduced by lowering OPC consumption, for example, by using industrial by-products such as blast furnace slag (BFS) or fly ash (FA) as supplementary cementitious materials in conventional concrete. Another alternative is alkali-activated concrete (AAC), for which OPC paste is completely substituted by an alternative, alkali-activated binder. Alkali-activated binder is formed by the reaction between a precursor (alumina- and silica-containing solids) and an alkaline solution. The industrial by-products (e.g., BFS, FA) or treated waste materials can be used as precursors.

Although AAC seems to have promising qualities for structural application in terms of sustainability, worldwide use is not yet established. One of the reasons for this is the fact that there are no available regulations or Codes to apply it. Though in Russia and Ukraine AAC was used in buildings already early last century, in the following decades there was not a lot of progress in the research field. The material is still relatively new and there is lack of experience with its application. The Codes that are used for conventional concrete may not be directly applicable for AAC. For OPC concrete, the Design Codes are based on compressive strength at 28 days, and most other mechanical properties are based on this strength. After 28 days, the compressive strength, and with that all other properties, increase in time. For AAC it is not yet clear if the relations and assumptions that are valid and proven for OPC concrete are applicable. In that respect it can be mentioned that mechanical properties of AAC vary a lot, depending on the wide range of available mixture compositions and curing conditions. Furthermore, most of the research conducted so far is on the paste or mortar level and limited research has been conducted regarding the structural properties of AAC. And finally, the long-term performance of AAC is scarcely investigated. Related to that, a few researchers reported a decrease of strength or stiffness over time for AAC mixtures that contain BFS. Collins and Sanjayan[5] were the first that reported a strength reduction for alkali-activated slag (AAS) concrete. In their research, AAS concrete cylinders exposed to 50% RH and 23°C directly after unmoulding at the age of 1 day, lost 17% of their compressive strength between 56 days and 1 year. On the other hand, sealed and bath cured samples did not exhibit this reduction and even showed an increase of compressive strength over time. Wardhono et al.[6] reported a reduction of flexural strength and elastic modulus for AAS concrete, while compressive strength was approximately constant over time. The elastic modulus of AAS concrete showed a 43% drop from 28 to 540 days. These samples were water-cured for 6 day after being demoulded and were subsequently kept at room temperature until being tested. However, for alkali-activated FA concrete, heat-cured at 80°C for 24 hr and subsequently kept at room temperature until testing, Wardhono et al.[6] did not observe a decrease of properties over time. It is expected that the reported phenomena of a decrease in material properties might be related to the material composition, for example, presence of BFS, and/or the type of curing conditions, for example, presence of water. Based on this information, there is no certainty about strength and stiffness development of AAC over time and it is not clear if the compressive strength at 28 days can be used as a safe reference for design. Besides the limited amount of knowledge about the performance of AAC and material-related properties over time, almost no research has been conducted regarding the time-dependent structural behavior of the reinforced AAC.

To the authors' opinion the reported decrease in material properties[5,6] should first be well-understood before upscaling structural applications of AAC. The intention of this research is to make first steps towards a better understanding of this phenomenon and its effect on structural behavior of reinforced AAC. This paper reports the results of an experimental research[7] that has been carried out to investigate the time-dependent behavior of a range of mechanical properties of two mixtures of AAC (BFS system and blended BFS/FA system) and the flexural behavior of corresponding reinforced AAC beams. The properties assessed were compressive strength, tensile splitting strength and elastic modulus up to 695 days, flexural strength up to 91 days, while furthermore the structural capacity and cracking patterns of reinforced AAC beams up to 151 day were investigated.

## 2 | EXPERIMENTAL PROCEDURE

### 2.1 | Materials and mixture designs

Based upon the results in literature,[5,6] it was hypothesized that the amount of BFS in the binder of AAC might play a role in the observed decrease of properties over time. Therefore, in this research, the development of strength and stiffness was investigated for two AAC mixtures with a difference in amount of BFS in the binder. Mixtures S100 and S50, characterized by a 0:100 and 50:50 FA/slag precursor binder ratio respectively were used. Table 1 shows the AAC mixture compositions used in this research. These mixtures were developed in previous studies at the TU Delft.[8–11] FA and BFS were the applied precursors and their chemical compositions are shown in Table 2. The precursors were activated by alkaline activator made of 4-M sodium-hydroxide (NaOH/4 M) and waterglass ($Na_2SiO_3$). Weight

ratio between (NaOH/4 M) and waterglass was 1. The activator was cooled down to room temperature before preparation of the concrete. Both AAC mixtures were characterized by a solution/binder ratio of 0.53. No admixtures (retarders or superplasticizers) were added.

For casting of the reinforced AAC beams, wooden molds and reinforcement were prepared. All reinforced beams are characterized by a tensile reinforcement ratio of 0.61% and are desinged to fail in flexure under four point bending.

## 2.2 | Specimen preparations and casting

The experimental program is shown in Figure 1. The preparation of all specimens was divided over four different days, to spread the amount of tests in the weeks after the castings. For the material tests, mixing of 25 L concrete batches was carried out using a 40 L concrete mixer. Similarly, using 40 L concrete mixer, S100 reinforced beams were casted in batches of 25 L, because of the fast hardening time of the material. A 220 L mixer was used for casting S50 reinforced beams, in batches of 100 L. Three cubes of 150 × 150 × 150 $mm^3$ were casted together with reinforced beams as a reference and to determine the compressive strength when testing the beam.

In the mixing process, the dry materials (BFS and/or FA, fine and coarse aggregates) were firstly mixed for 3 min. Meanwhile, the sodium-hydroxide solution was added to the waterglass and continuously stirred. Then, the alkaline activator was added to the dry mix, and mixing continued for another 3 min until the mixture was well-mixed. The initial setting time of the S50 mix was about 20 min. The S100 mixture had almost no workability, it started hardening immediately. The AAC was then poured in the preoiled molds that were positioned on the vibrating table. For the first casted batches, oil was used, but during later castings Vaseline was applied, because it proved to be easier during unmoulding. When all molds were half full, the AAC was vibrated for about 20 s. After this, the rest of the AAC was poured in the molds and another 20 s of vibrations were applied. The molds were covered with plastic film. After 1 day of hardening, all specimens were unmoulded and placed in the fog room where they have been cured (20°C and 95% RH) for 28 days. After the 28-day curing period, all the specimens but two, were moved from the curing room to laboratory conditions (20°C and 55% RH). One sample of each S50 and S100 was left in the curing room until the age of 91 days.

**TABLE 1** Alkali-activated concrete mixtures[8]

| | S50 | S100 |
|---|---|---|
| For 1 $m^3$ concrete: | [kg] | [kg] |
| Low calcium fly ash (FA) | 200 | 0 |
| Blast furnace slag (BFS) | 200 | 400 |
| Sand (0–4 mm) | 784 | 784 |
| Gravel (4–8 mm) | 435,5 | 435,5 |
| Gravel (8–16 mm) | 522,5 | 522,5 |
| Alkaline solution | 212 | 212 |
| Solution/binder ratio | 0.53 | 0.53 |

*Note:* S50 and S100 are labels for AAC mixtures.

## 2.3 | Testing

### 2.3.1 | Material properties

Flexural strength was determined by a three-point bending test in accordance with NEN-EN 14651 + A1, except for the fact that the specimen size was 100 × 100 × 400 $mm^3$ instead of 150 × 150 × 550–700 mm,[3] as specified in the NEN-standard. The tests have been performed using an Instron machine, with the controlled crack opening at speed of 0.5 μm/s. In all samples a notch of 25 mm was made at midspan, using wet-sawing. After this, the samples were dried for at least 6 hours before testing.

The compressive strength test was performed in accordance with NEN-EN 12390–3, but on cube specimens of 100 × 100 × 100 $mm^3$ instead of 150 × 150 × 150 $mm^3$. These cubes were sawn from the specimens that were first used for flexural tests (see Figure 1), using wet-sawing. Compressive strength tests were performed using a CYBER-TRONIC machine, with a loading rate of 6.5 kN/s. The tensile splitting tests were performed in accordance with NEN-EN 12390–6, but instead of cylindrical specimens, cube specimens of 100 × 100 × 100 $mm^3$ were used. The cubes were sawn from the specimens that were first used for flexural tests, using wet-sawing. Tensile splitting strength tests were performed using a CYBER-TRONIC machine, with a loading rate of 6.5 kN/s.

Elastic modulus was determined in accordance with ISO 1920-10:2010. The specimen size was 100 × 100 × 400 $mm^3$, so the height/width ratio is 4. In order to have more realistic practical conditions, the specimens were not re-immersed in water for 12 hours, before testing, as

**TABLE 2** Chemical composition of BFS and FA used, based upon X-ray fluorescence results by Nedeljković et al[12]

| [%] | $SiO_2$ | $Al_2O$ | CaO | Mg | $Fe_2O$ | $SO_3$ | $Na_2$ | $K_2$ | TiO | $P_2O$ | L.O.I. |
|---|---|---|---|---|---|---|---|---|---|---|---|
| BFS | 34.40 | 11.53 | 39.17 | 7.81 | 1.42 | 1.60 | 0.23 | 0.58 | - | - | 1.15 |
| FA | 54.28 | 23.32 | 4.23 | 1.62 | 8.01 | 0.64 | 0.85 | 1.97 | 1.23 | 0.54 | 3.37 |

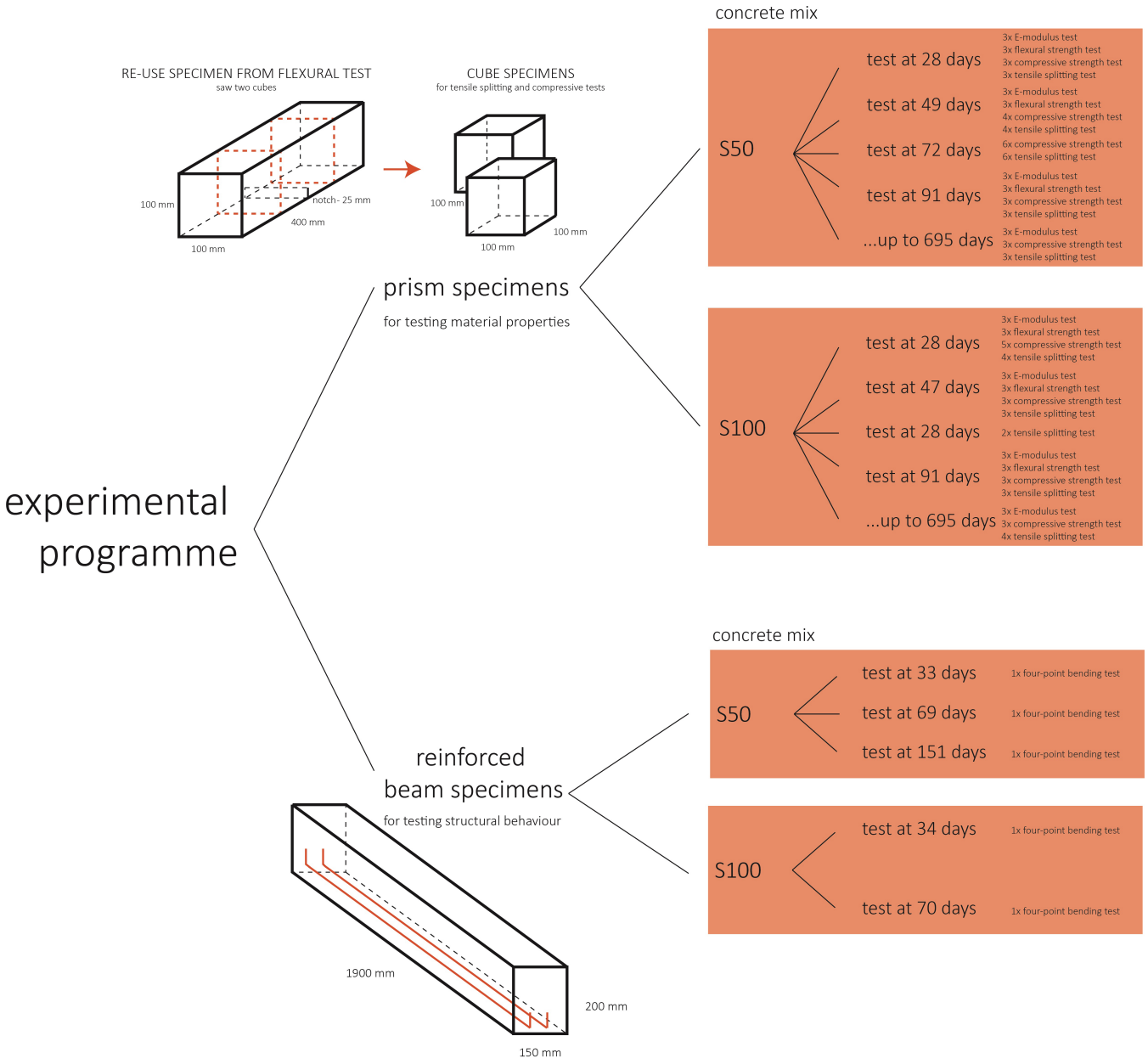


**FIGURE 1** Overview of experimental programme

indicated by standard. The tests were performed using a TONI-BANK machine with a speed of 0.001/s.

Environmental Scanning Electron Microscope (ESEM), Philips-XL30-ESEM, was used to observe microstructural changes. Thin sections for the microscopic study were prepared by sawing small sections from the specimens used for elastic modulus test. The dimensions of these sections were $40 \times 40$ mm$^2$, with a thickness of approximately 10 mm.

### 2.3.2 | Four-point bending tests

Four-point bending tests of all reinforced AAC beams were performed in a test machine with a capacity of 100 kN. The beams were simply supported over a span of 1,500 mm and subjected to two concentrated loads placed symmetrically on the span. The distance between the loads was 500 mm. Linear variable differential transformers (LVDTs) were placed at several locations on the beam, three at the bottom, one at the side to measure elongations and one at the bottom to measure vertical deflection. For measuring the vertical deflection, a wooden substructure was attached along the beam, spanning from support to support at the height of the neutral axis (Figure 2). The loading of the specimens was controlled by the displacement of the jack with a speed of 0.01 mm/s. After every step of 5 kN, the loading was stopped, cracks were marked and measured and photos were

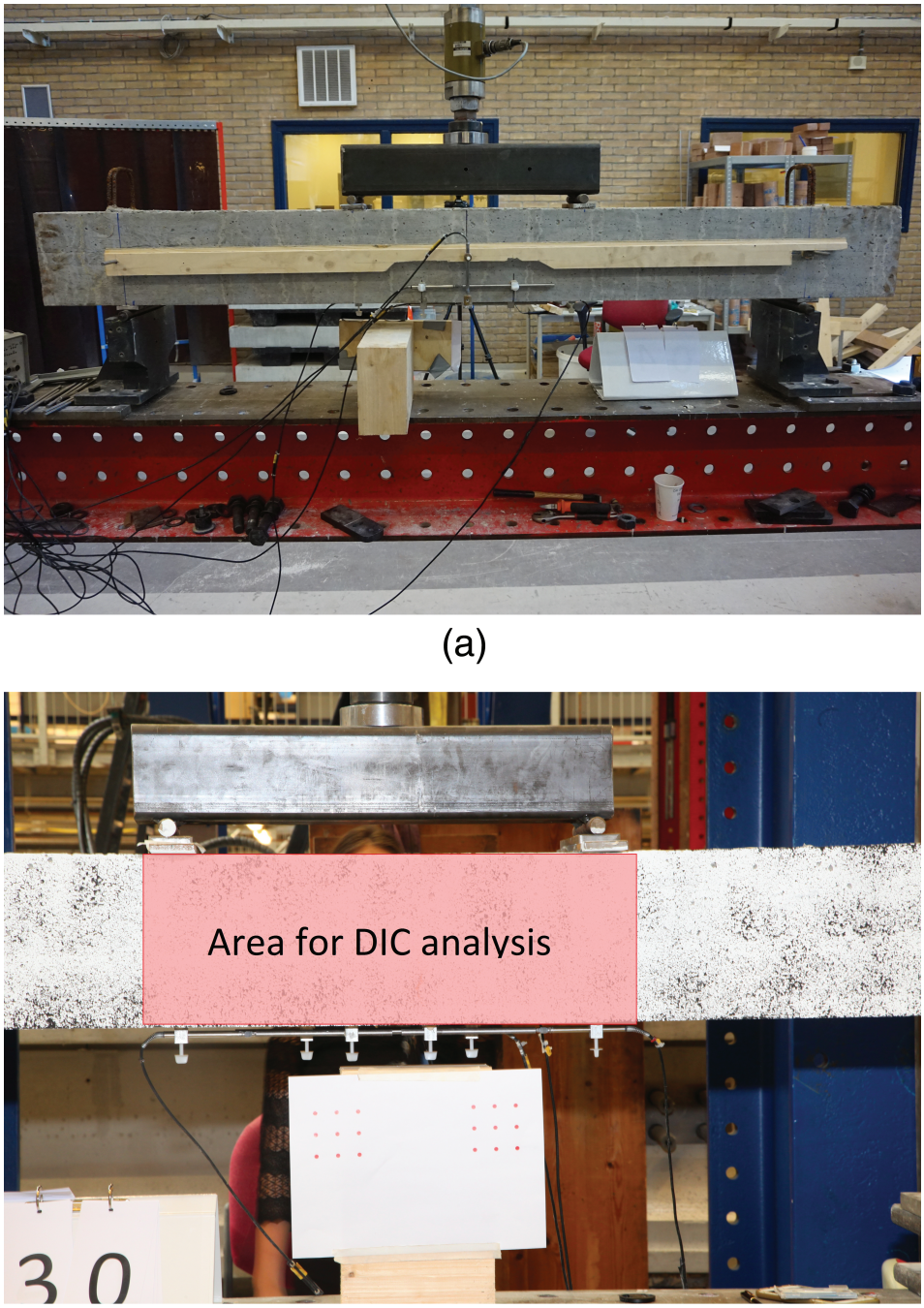


**FIGURE 2** Four-point bending test set-up (a) and painted part of the surface at the other side, used for DIC measurements (b)

taken. When the force reached approximately 60 kN, the speed was increased to 0.05 mm/s.

During this test digital image correlation (DIC) technique is used for capturing deformations in the reinforced AAC beam (Figure 2b). This is a non-contact optical method that employs tracking and image registration techniques for accurate two-dimensional measurements of changes in images. This allows calculating deformation, displacement and strain on the observed surface. Details regarding this procedure can be found in references.[13–15] In this study, DIC was used to track crack development in the reinforced AAC and conventional concrete beams and to compare their structural behavior.

## 3 | EXPERIMENTAL RESULTS

### 3.1 | Mechanical properties – Time-dependent behavior

Table 3 displays an overview of the mechanical properties that were obtained for the S100 mixture (100% slag, no FA).

**TABLE 3** Mechanical properties of S100 mixture (100% slag, no fly ash)

| S100 | Compr. Strength [MPa] | | | Elastic modulus [GPa] | | | Tens. Spl. Strength [MPa] | | | Flexural strength [MPa] | | |
|---|---|---|---|---|---|---|---|---|---|---|---|---|
| Days | | SD | Average | | SD | Average | | SD | Average | | SD | Average |
| 28 | 91.63 | 1.76 | 93.45 | | 0.41 | 32.96 | 5.46 | 0.27 | 5.38 | | 0.58 | 6.22 |
| | 92.75 | | | 32.50 | | | 5.23 | | | 6.55 | | |
| | 92.84 | | | 33.29 | | | 5.11 | | | 5.56 | | |
| | 96.31 | | | 33.08 | | | 5.72 | | | 6.57 | | |
| | 93.74 | | | | | | | | | | | |
| 47 | 99.84 | 3.36 | 95.98 | 32.41 | 1.23 | 31.91 | 5.39 | 0.35 | 5.42 | 6.87 | 0.25 | 6.60 |
| | 93.71 | | | 30.51 | | | 5.78 | | | 6.39 | | |
| | 94.39 | | | 32.82 | | | 5.09 | | | 6.53 | | |
| 74 | | | | | | | 4.79 | 0.90 | 5.43 | | | |
| | | | | | | | 6.07 | | | | | |
| 91 | 94.56 | 4.63 | 97.96 | 30.41 | 1.89 | 28.55 | 4.67 | 0.09 | 4.77 | 6.06 | 0.26 | 5.76 |
| | 96.09 | | | 28.62 | | | 4.84 | | | 5.63 | | |
| | 103.23 | | | 26.63 | | | 4.80 | | | 5.60 | | |
| 193 | 81.97 | 9.40 | 92.71 | 28.04 | 1.62 | 26.22 | 4.81 | 0.13 | 4.97 | | | |
| | 99.42 | | | 24.93 | | | 5.09 | | | | | |
| | 96.73 | | | 25.68 | | | 4.91 | | | | | |
| | | | | | | | 5.05 | | | | | |
| 695 | 90.84 | 0.59 | 91.27 | 24.16 | 2.70 | 25.46 | 4.91 | 0.34 | 5.13 | | | |
| | 91.94 | | | 23.66 | | | 5.32 | | | | | |
| | 91.03 | | | 28.56 | | | 4.78 | | | | | |
| | | | | | | | 5.50 | | | | | |

Note that flexural strength was measured only until the age of 91 days. In Table 4, all results for the S50 mixture (50% slag, 50% FA) are reported. As can be seen, for the elastic modulus, tensile splitting strength and flexural strength a decrease over time is found for both AAC mixtures.

### 3.1.1 | Compressive strength

Figure 3a displays the development of compressive strength for both S50 and S100. The compressive strength results for S100 show that, although a slight increase of 4% can be observed at 91 days, the 193 days and 2 years strengths are comparable and slightly less than the 28 days strength. Similarly for the S50 mixture, although a slight decrease of approximately 4% is found at 91 days, compressive strength seems to have a relatively stable trend up to the age of 2 years. So, the compressive strength of both mixtures was more or less constant between 28 and 2 years.

### 3.1.2 | Elastic modulus

In Figure 3b the development of elastic modulus for both mixtures is presented. A decrease over time can be observed, being approximately 13% for the S100 and 30% for the S50 mixture at the age of 91 days. Until the age of 2 years, elastic moduli further reduce, and are 23% and 35% lower compared with those at 28 days for S100 and S50 mixes respectively.

### 3.1.3 | Flexural strength

Figure 3c shows the development of flexural strength over time for both AAC mixtures. The flexural strength of the S100 decreased 7% between 91 and 28 days. For S50, this decrease is higher and about 15%.

### 3.1.4 | Tensile splitting strength

An overview of the development of tensile splitting strength for both mixtures is shown in Figure 3d. It is clear that both AAC mixtures show a decrease of tensile splitting strength over time. The tensile splitting strength of S100 dropped with 11% between 91 and 28 days. For S50, this decrease is about 22%. However, at the age of 193 and 695 days, mix S100 shows an increase compared to 91 days values, whereas tensile splitting strength of mix S50 is approximately constant.

**TABLE 4** Mechanical properties of S50 mixture (50% slag, 50% fly ash)

| S50 | Compr. Strength [MPa] | | | Elastic modulus [GPa] | | | Tens. Spl. Strength [MPa] | | | Flexural strength [MPa] | | |
|---|---|---|---|---|---|---|---|---|---|---|---|---|
| Days | | SD | Average | | SD | Average | | SD | Average | | SD | Average |
| 28 | 76.13 | 2.32 | 75.25 | 26.57 | 0.39 | 26.42 | 4.60 | 0.40 | 4.67 | 4.56 | 0.14 | 4.66 |
| | 77.00 | | | 25.98 | | | 4.30 | | | 4.61 | | |
| | 72.62 | | | 26.73 | | | 5.10 | | | 4.82 | | |
| 49 | 76.46 | 5.34 | 71.54 | 21.44 | 0.08 | 21.40 | 3.90 | 0.20 | 4.02 | 4.43 | 0.20 | 4.59 |
| | 64.88 | | | 21.46 | | | 3.88 | | | 4.52 | | |
| | 75.19 | | | 21.31 | | | 3.99 | | | 4.82 | | |
| | 69.62 | | | | | | 4.30 | | | | | |
| 72 | 74.50 | 4.87 | 72.77 | | | | 3.88 | 0.24 | 3.95 | | | |
| | 77.09 | | | | | | 3.72 | | | | | |
| | 63.40 | | | | | | 3.97 | | | | | |
| | 72.10 | | | | | | 3.88 | | | | | |
| | 75.42 | | | | | | 4.42 | | | | | |
| | 74.12 | | | | | | 3.85 | | | | | |
| 91 | 74.89 | 3.39 | 71.77 | 19.28 | 0.56 | 18.36 | 3.58 | 0.24 | 3.60 | - | 0.20 | 3.93 |
| | 74.11 | | | 18.00 | | | 3.50 | | | 4.16 | | |
| | 68.99 | | | 18.15 | | | 3.99 | | | 3.88 | | |
| | 73.53 | | | 17.90 | | | 3.32 | | | 3.77 | | |
| | 67.31 | | | 18.45 | | | 3.43 | | | - | | |
| | | | | | | | 3.76 | | | - | | |
| 195 | 76.31 | 1.86 | 74.22 | 17.29 | 0.12 | 17.41 | 3.36 | 0.31 | 3.65 | | | |
| | 73.62 | | | 17.54 | | | 3.62 | | | | | |
| | 72.73 | | | 17.39 | | | 3.97 | | | | | |
| 695 | 70.39 | 1.92 | 71.37 | 17.04 | 0.23 | 17.23 | 3.49 | 0.11 | 3.52 | | | |
| | 71.43 | | | 17.17 | | | 3.41 | | | | | |
| | 74.03 | | | 17.49 | | | 3.49 | | | | | |
| | 69.63 | | | | | | 3.68 | | | | | |

## 3.2 | Comparison 28-day properties of the investigated AAC with OPC concrete properties

Table 5 shows a comparison between the tested properties for AAC and estimated properties for OPC concrete with similar compressive strength, where the properties of OPC concrete are estimated based on Eurocode 2 equations.

It is clear from Table 5 that tensile splitting strength ($f_{ct,sp}$) can be estimated quite well using Eurocode 2. The value for S50 is overestimated by about 8% using the EC2 equations, which is in this range of variations regularly found. For elastic modulus, for S50, the results based upon experiments are 30% lower than the values common for regular OPC concrete. It can be concluded that applying EC2 relation valid for regular OPC concrete gives overestimation of elastic modulus of AAC.

Although several researchers[4,16,17] reported that the flexural and tensile strength of AAC (e.g., for BFS systems and blended BFS/FA and BFS/metakaolin systems) is significantly higher than the one expected from the codes on OPC concrete, this is not the case for the experimental results that were obtained in this research. Figure 4 shows the relationship between flexural and compressive strength, for different types of AAC.[4] The results from this research have also been added. It is clear that the ratio between flexural strength and compressive strength is comparable to OPC concrete, for the chosen mixtures and curing conditions. However, the wide variety in reported results proves that this is not necessarily the case for all AAC mixtures.

## 3.3 | Flexural behavior of reinforced beams

Table 6 gives an overview of the results of the four-point bending tests on reinforced beams performed at different

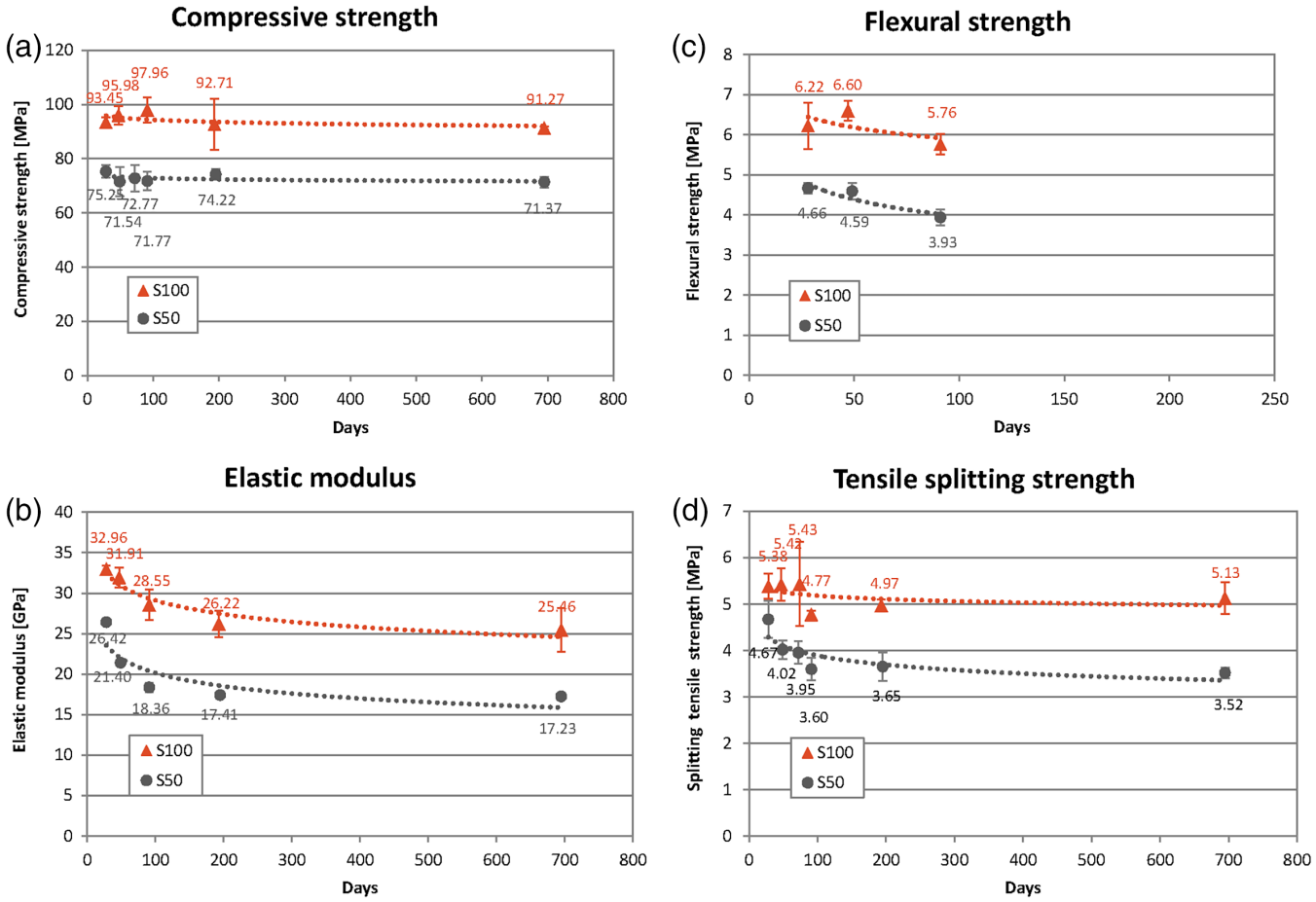


**FIGURE 3** Development of compressive strength (a), elastic modulus (b), flexural strength (c) and tensile splitting strength (d) over time for the investigated alkali-activated concrete

**TABLE 5** Comparison of mechanical properties according to equations in Eurocode 2 and measured properties for the S50 and S100 specimens at 28 days

| COMPARISON | OPCC codes | | S50 test results | | % | OPCC codes | | S100 test results | | % |
|---|---|---|---|---|---|---|---|---|---|---|
| $f_{cm\_cube\&\$\$\$;}$ | 75.3 | MPa | **75.3** | **MPa** | | 93.5 | MPa | **93.5** | **MPa** | |
| $f_{cm} = 0.8 * f_{cm\_cube\&\$\$\$;}$ | 60.2 | MPa | - | **MPa** | | 74.8 | MPa | - | **MPa** | |
| $f_{ccm} = 2.12 * \ln\left(1 + \frac{f_{cm}}{10}\right)$ | 4.1 | MPa | - | **MPa** | | 4.5 | MPa | - | **MPa** | |
| $f_{ct\_sp} = \frac{f_{ccm}}{0.9}$ | 4.6 | MPa | **4.2** | **MPa** | **−8.5%** | 5.0 | MPa | **5.4** | **MPa** | **6.9%** |
| $E_{cm} = 22000\left[\frac{f_{cm}}{10}\right]^{0.3}$ | 37.7 | GPa | **26.4** | **GPa** | **−30.0%** | 40.2 | GPa | **33.0** | **GPa** | **−18.0%** |

*Note:* The bold values are experimentally obtained mechanical properties for AAC mixes.

ages. The four-point bending tests on reinforced AAC beams exhibited flexural failure after reinforcement yielding for all five beams. As a final failure, for three beams, reinforcement failure was observed, while for the S50 beams tested at 69 and 151 days, crushing of the AAC in the compression zone was observed. The location of the failure zone was in the constant bending moment zone (between the loading points) for all beams, as expected. In all cases, the cracks at the mid-span widely opened near failure.

Figure 5a,b shows the load versus mid-span deflection curves for the S50 and S100 beams, respectively, tested at different ages. The mid-span deflection was measured using an LVDT, however, because it was out of range during the test, it was chosen to plot the deformation of the jack. It can be observed that the decrease of the elastic modulus and the tensile splitting strength did not have a significant influence on load carrying capacity of the reinforced AAC beams.

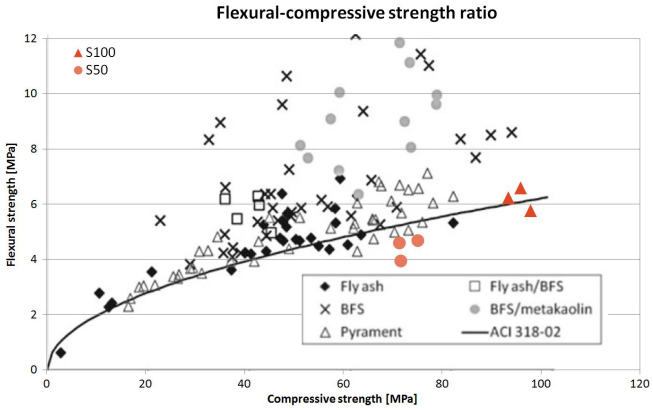


**FIGURE 4** Relationship between flexural and compressive strength of alkali-activated concretes, synthesized from various precursors as marked, at ages between 4 hr and 1 year, with the relationship for OPC concretes as specified in ACI 318–02 shown for comparison (Provis & van Deventer, 2014,[4] p. 283). The results from this research have been added in orange, for both S50 and S100, at the age of 28 days

## 3.4 | Flexural behavior of reinforced beams – OPC concrete versus AAC

In Figure 5a, the load deflection curves for S100 beam and control OPC concrete beam[18] tested at the age of 33 days are presented. The reinforced OPC beam has exactly the same dimensions, reinforcement and cover as the AAC beams, but lower compressive strength (45 MPa). The structural behavior of these two beams is compared due to their similar elastic modulus, namely 33 GPa as tested for S50 and 32 GPa as predicted by EC2 equation for the applied conventional concrete. Crack development in reinforced AAC beam is also examined during the loading. In the load–deflection curves (Figure 6), points are chosen for which the snapshots of the crack history are made. Strain fields, indicating crack development, as analyzed by DIC are presented in Figure 7. Similarly as commonly observed for reinforced concrete beams, also for AAC beams three phases could be distinguished: precracking phase, crack formation phase and yielding of the steel (fully developed crack pattern) followed by the failure of the beam.

The crack spacing is similar for both beams. The final deflection at failure for the reinforced AAC is significantly higher compared to that of conventional reinforced concrete beams, similarly as found by Shah & Shah.[19] Furthermore, due to the higher compressive strength of the AAC compared to that of the conventional concrete, the capacity of the reinforced AAC is higher.

Figure 8 shows the crack patterns at the failure of an OPC concrete control beam[18] compared to that of all the AAC beams. It can be observed that the crack patterns of reinforced AAC, that is, S50 and S100 reinforced beams, are comparable to that of the regular OPC concrete beam.

Figure 9a,b shows an overview of the load-deflection behavior and the crack width development during the four-point bending tests, for all AAC beams and the OPC concrete control beam. Structural behavior and cracking patterns

**TABLE 6** Results of four-point bending tests on AAC

| Beam | Testing age [days] | Tens. Reinf. Ratio [%] | Compr. Strength [MPa] | Compr. Strength Average | Failure load [kN] | Max. Deflection jack [mm] | Max. Deflection LVDT01 [mm] | Ultimate bending moment [kNm] |
|---|---|---|---|---|---|---|---|---|
| S50 | 33 | 0.61 | 80.32 | 75.1 | 67.4 | 32.5 | 27.4 | 16.9 |
| | | | 78.31 | | | | | |
| | | | 66.62 | | | | | |
| S50 | 69 | 0.61 | 81.73 | 77.1 | 58.8 | 35.2 | 34.3 | 14.7 |
| | | | 70.87 | | | | | |
| | | | 78.61 | | | | | |
| S50 | 151 | 0.61 | 78.21 | 78.7 | 69.7 | 40.7 | 43.2 | 17.3 |
| | | | 79.22 | | | | | |
| S100 | 34 | 0.61 | 91.20 | 86.6 | 67.6 | 30.1 | 33.1 | 16.9 |
| | | | 81.94 | | | | | |
| S100 | 70 | 0.61 | 88.04 | 83.7 | 66.3 | 37.4 | 35.0 | 16.6 |
| | | | 71.24 | | | | | |
| | | | 91.79 | | | | | |
| *OPC concrete* | *33* | *0.61* | | *45.7* | *59.1* | *17.7* | *10.8* | *14.8* |

*Note:* The table shows results for both S100 (100% slag) and S50 (50% slag and 50% fly ash) beams and a regular OPC concrete beam (results by[18]).

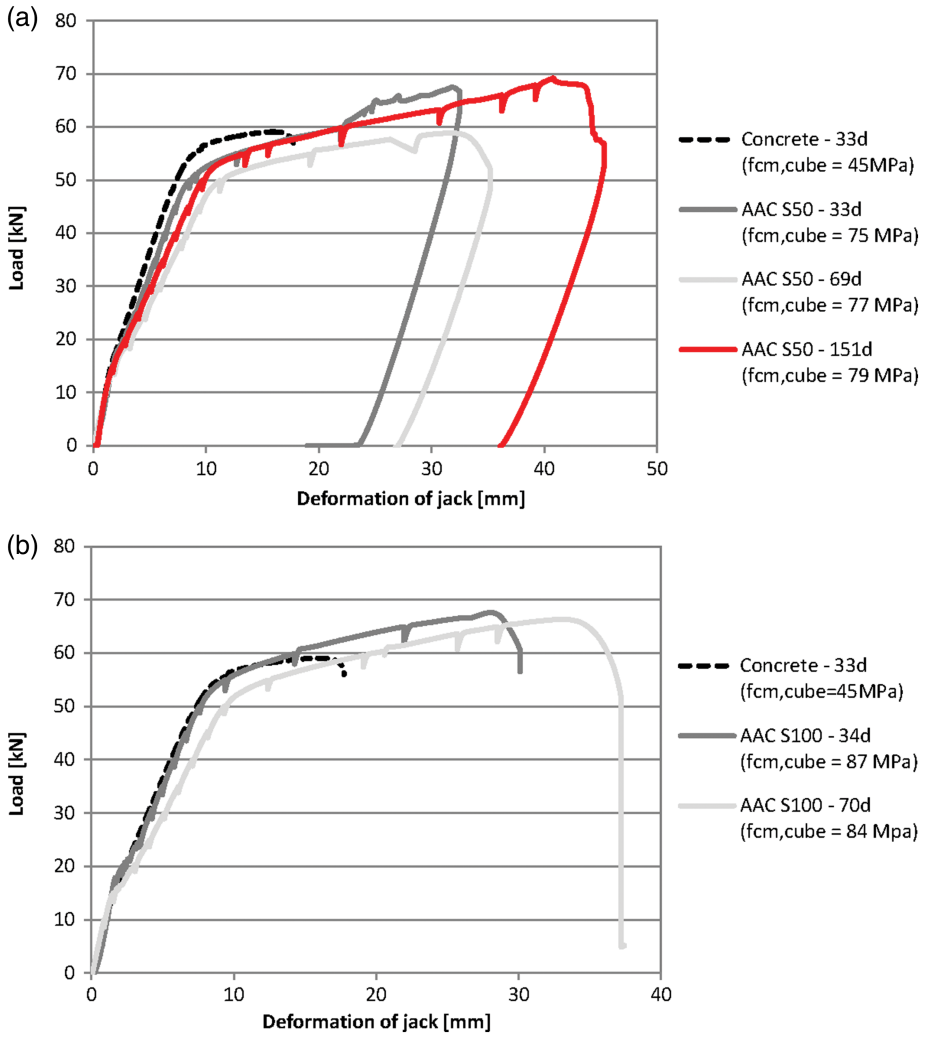


**FIGURE 5** Load-deformation curves resulting from four-point bending tests on OPC concrete and S50 (a) and S100 (b)

(crack spacing and width), were found to be similar for reinforced AAC and conventional concrete, similarly as found by.[20]

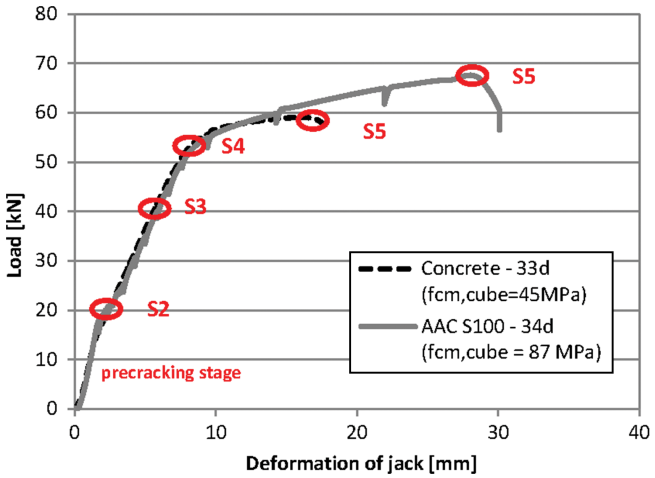


**FIGURE 6** Load displacement curves for AAC S100 and conventional concrete, both tested at the age of 33 days

## 4 | DISCUSSION

Figure 10a shows the relative value of compressive strength, tensile splitting strength and elastic modulus for S50, compared to that one of 28 days. For tensile splitting strength and elastic modulus a decrease over time is found, while the compressive strength stayed more or less constant. It can also be seen that the reduction of properties is stabilizing over time.

In Figure 10b, the relative change of the properties is plotted for S100 (100% slag). Also for S100, the highest decrease over time is observed for the elastic modulus. S50 shows a higher degree of decrease over time than S100 for tensile splitting strength and elastic modulus. The results show a higher decrease in material properties for the S50 with less amount of BFS than in the S100, so there is probably no direct relation between the decrease in material properties and the amount of BFS in the binder.

The observed trend in properties is consistent for both S50 and S100. Compressive strength shows no decrease,

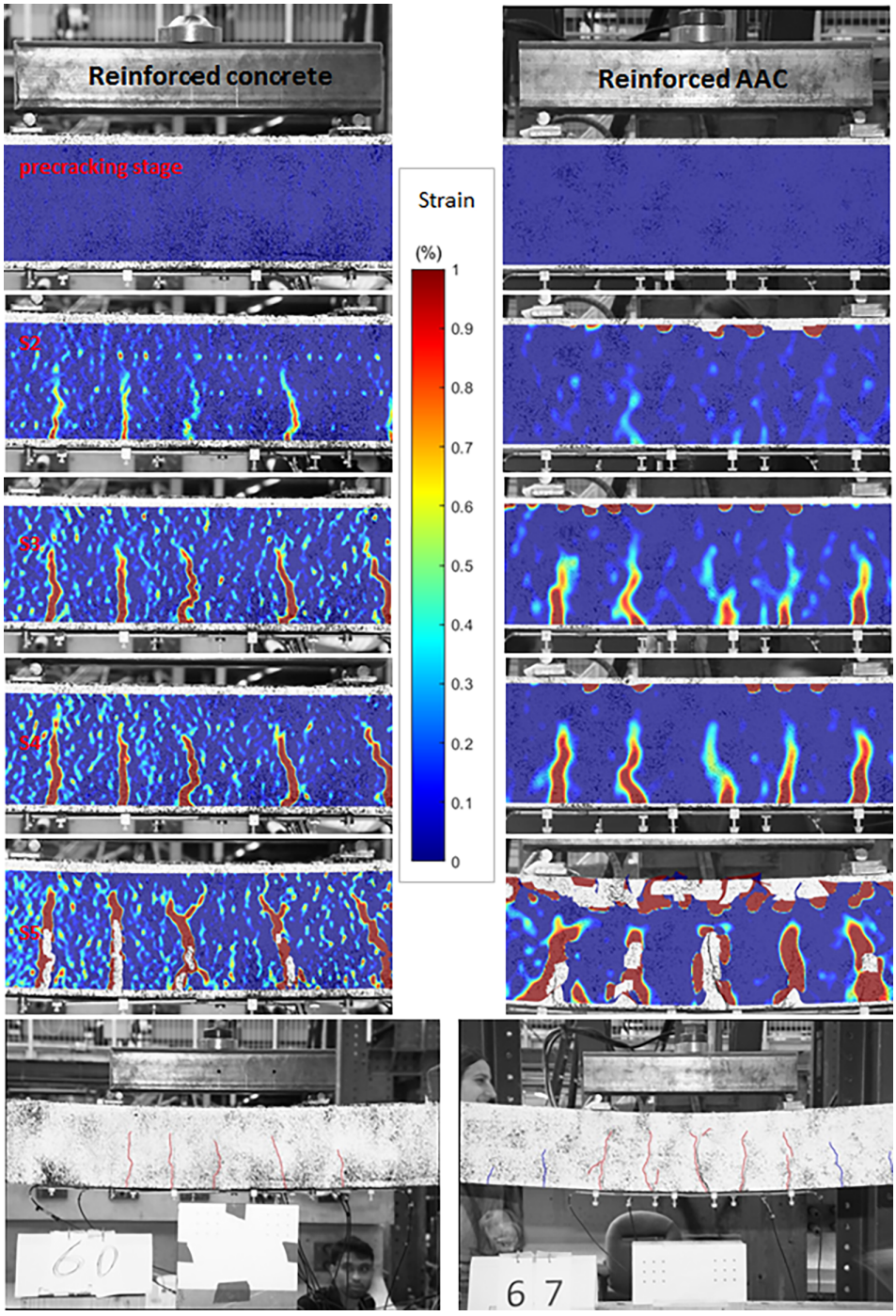


**FIGURE 7** Strain field concentrations indicating crack developments in AAC (right) and conventional reinforced concrete (left)

while tensile splitting strength and elastic modulus, shows a decrease over time, being the highest for the elastic modulus. This is consistent with the few results reported in literature, that also show the biggest decrease for elastic modulus and (almost) no decrease for compressive strength.[6] The decrease is stabilizing and becoming smaller after the age of 91 days for mix S50 and after the age of 193 days for mix S100.

As already noted, the decrease of properties over time cannot be directly related to the amount of slag in the binder, as hypothesized. Another reason might be that it is related to the curing conditions. All these samples were wet-cured for 28 days and then exposed to laboratory conditions until the age of testing, that is, 28, 56, 91, 193 and 695 days. It might be that exposing the samples to dry after the wet-curing period has influence on the development of the measured properties, for example, due to differential shrinkage. For both AAC mixtures (S50 and S100), one sample was left in the curing room (20°C and 95% RH) for 92 days and then tested. The results of the elastic modulus tests on these samples are shown in Figure 11 and are compared to the elastic moduli measured at the age of 28 days and to that in exposed samples at different ages.


**FIGURE 8** Crack patterns in reinforced beams, photos taken after failure. Dotted lines indicate the constant moment zone

Figure 11 shows that for the samples continuously kept in the curing room for 92 days, the elastic modulus increased with more than 15% compared to 28 days values, both for S50 and S100 mixtures. These results indicate that the drop of tensile splitting strength and stiffness, that has been previously observed (Figure 3), might be related to the process of drying. Samples that were taken out of the curing room after 28 days of wet-curing show a decrease over time, while samples that were wet-cured for 92 days and tested at the age of 92 days, show an increase when compared to the 28 day properties.

After taking the 92-day-cured samples S50 and S100 out of the moist curing, elastic modulus has been measured continuously at different ages to investigate if the same reduction trend, as noted previously for 28-day-cured examples, can be observed. An almost identical trend of decrease in E moduli can be observed after exposing both group of samples to laboratory conditions (50% RH, 20°C) (Figure 12). S50 shows a higher decrease of elastic modulus over drying time.

After taking the 92-day-cured samples out of the curing room, weight loss has been measured at different ages over time for both S50 and S100 samples. Figure 13a displays the measured weight loss, S50 shows a higher weight loss when compared to the S100 sample. Also, data for CEM III/B concrete is plotted in this graph,[21] showing that that the weight loss for the S100 sample is comparable to slag-rich CEM III/B concrete, whereas S50 loses more moisture. This larger loss of moisture for S50 over S100 is consistent with a higher decrease of respective elastic moduli over time.

In Figure 13b the relation between elastic modulus and weight loss is shown. A linear relation can be observed, which implies that there is a strong influence of moisture loss on the measured elastic modulus. This phenomenon is also observed in regular OPC concrete. Monteiro and Mehta[1] state that concrete specimens that are tested in wet conditions show about 15% higher elastic modulus than the corresponding specimens tested in a dry condition, disregarding any difference in mix proportions or curing age. Monteiro and Mehta[1] mentioned that the elastic modulus decreases because the interfacial transition zone loses strength due to microcracking. This could also be the case for the AAC. Yet, a bigger decrease than 15% is visible in the results on elastic modulus in this research.

A similar range of decrease of properties due to drying was also reported by Maruyama et al.[22] for various conventional concrete mixtures which, after sealed curing for 2 months, were exposed to different relative humidity conditions. After around 5 months, specimens stored in 40% and 60% relative humidity exhibited up to 30% and 15% decrease in elastic modulus and compressive strength, respectively and depending on the concrete mixture and type of aggregates used. In their research, stiffness and strength decrease was mainly attributed to crack formation, caused by the differences in the volume change between the aggregate and mortar.

In presented study, after around 5 months being exposed to the 50% relative humidity, AAC mixtures S50 and S100 exhibited 34% and 20% decrease in elastic modulus, which might be, up to a certain extent, in line with values reported for conventional concrete.[22] To investigate if any difference in microstructure was visible, it was decided to examine the microstructure of the

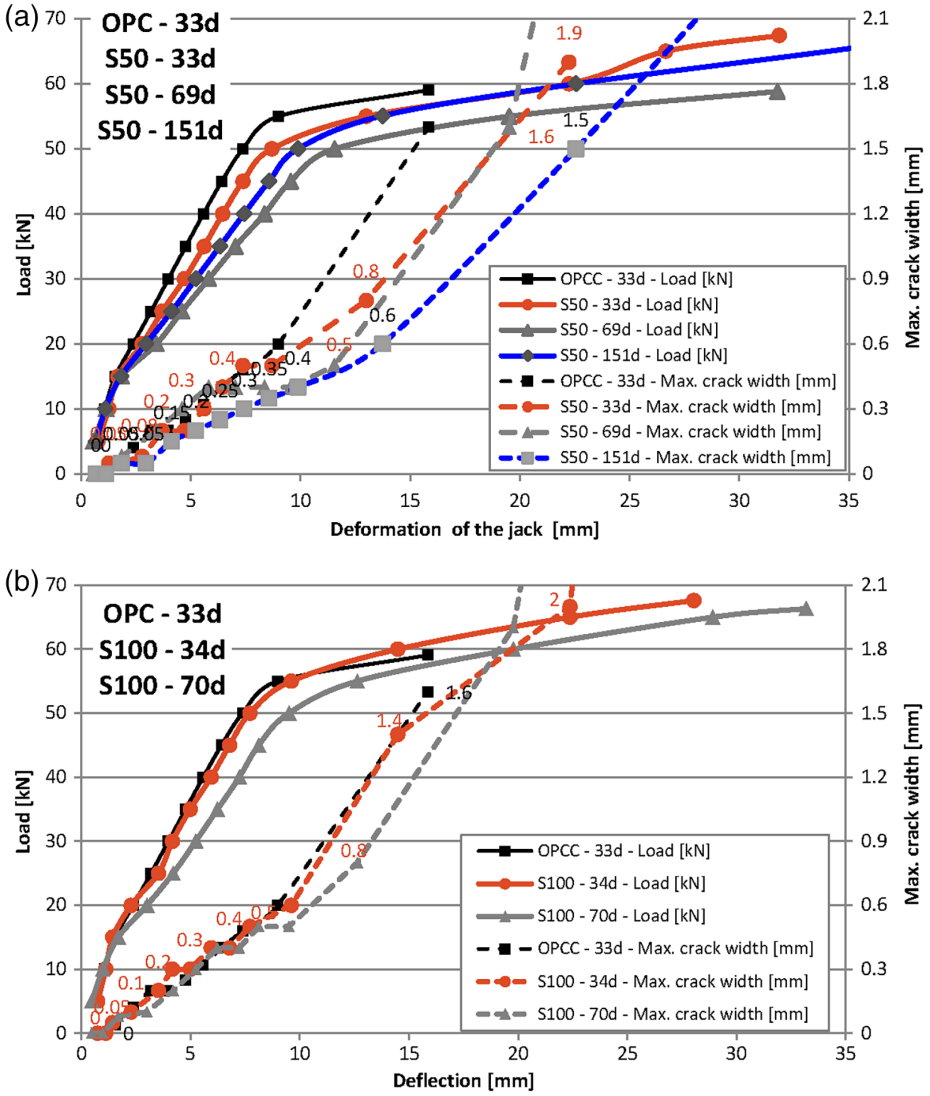


**FIGURE 9** Development of cracks during four-point bending tests on S50 beams at 33, 69 and 151 days (a) and S100 beams at 34 and 70 days (b). Results on a similar OPC concrete beam have also been plotted, data from Huang[18]

specimens with ESEM. Some ESEM images are shown in Figure 14. However, the ESEM analysis did not show clear differences between the samples that were cured for 28 days or 92 days. The images shows small microcracks (with a width of approximately 5 μm), both in the paste as well as in the interface between aggregate and paste. Also, there was no convincing difference between the microstructure at the edge (hypothetically more drying occurred there) and the inside of the sample. Some locations showed more microcracks, some spots almost none. To conclude, no significant difference in microstructure for samples with different curing duration and strength/stiffness development could be found with the ESEM analysis. However, with ESEM analysis only a very thin layer of the material (a few μm) is investigated and it might be that the surface is already affected during the preparation. Namely, during sawing and grinding, drying (cracks) may have already occurred in the wet-specimens that were cured for 92 days, resulting in similar images that were acquired for the dried specimens that were taken out of the curing at 28 days.

The acquired results indicate that the observed decrease of properties might be related to drying (moisture loss), but more research is needed to get a better understanding of the observed phenomenon. As long as decrease in properties is not caused by cracking, it might be that the observed decrease is only temporary (due to eigenstresses caused by shrinkage gradient), so examining the material behavior over a longer period of time could lead to other conclusions. In addition, it might be that different curing conditions (e.g., sealed curing instead of water curing) might be more preferential for these two AAC mixtures.

The observed decrease did not have significant influence on the structural behavior of the reinforced AAC. This might be because in the structural tests, only the small surface layer is affected and this has (almost) negligible effect in the larger reinforced elements.

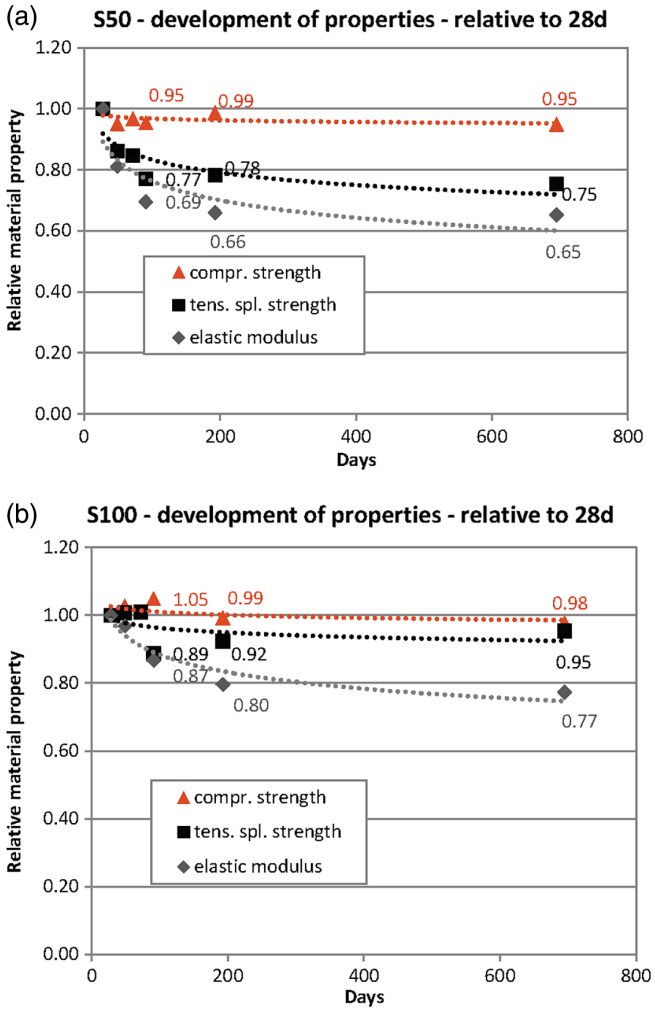


**FIGURE 10** Development of strength and stiffness over time until 695 days for S50 (a) and S100 (b) alkali-activated concrete mixtures

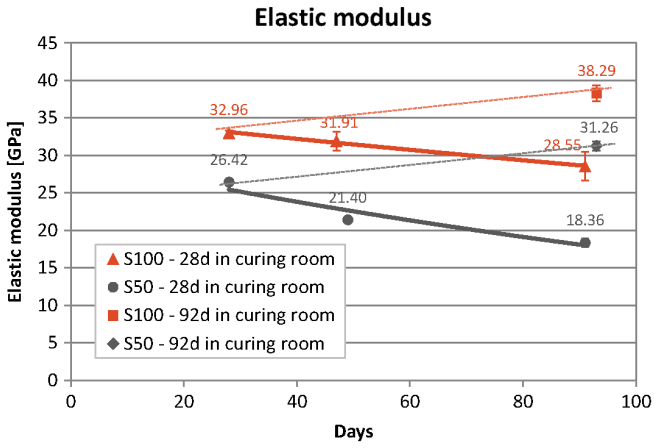


**FIGURE 11** Development of elastic modulus over time for alkali-activated concrete. The graph shows the development over time for both S100 (100% slag) and S50 (50% slag and 50% fly ash) mixtures

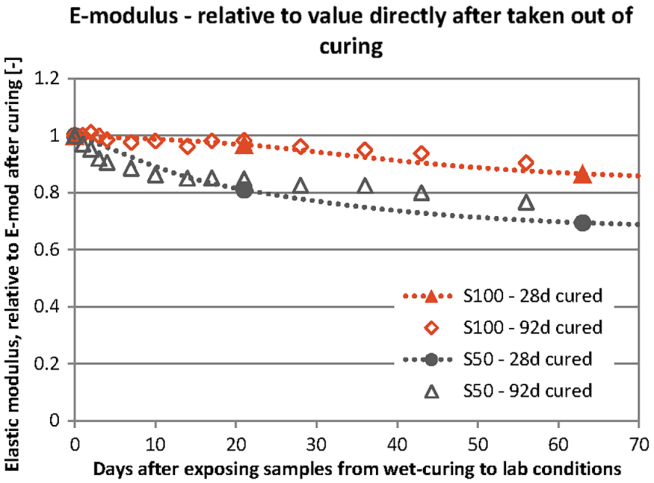


**FIGURE 12** Development of elastic modulus over time for alkali-activated concrete after curing for (20°C and 95% RH) for respectively 28 days and 92 days

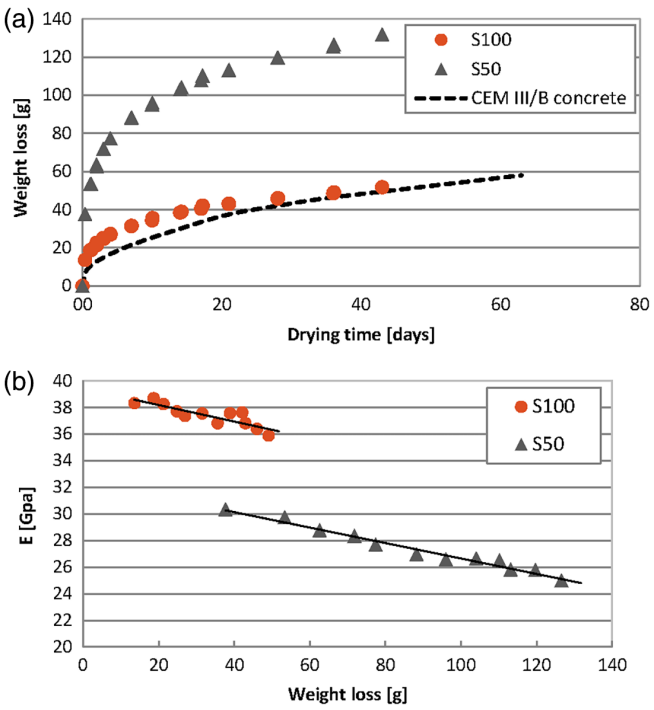


**FIGURE 13** Weight loss (a) and relationship between elastic modulus and weight loss (b) for one S50 and one S100 AAC sample that has been wet-cured (20°C and 95% RH) for 92 days

## 5 | SUMMARY AND CONCLUSIONS

The main goal of this research was to get insight in the development of strength and stiffness over time for AAC containing BFS and FA and its structural behavior over time. The reason was that sometimes a decrease in properties was reported in literature for AAC. Based on the test results, the following conclusions can be drawn from this research:

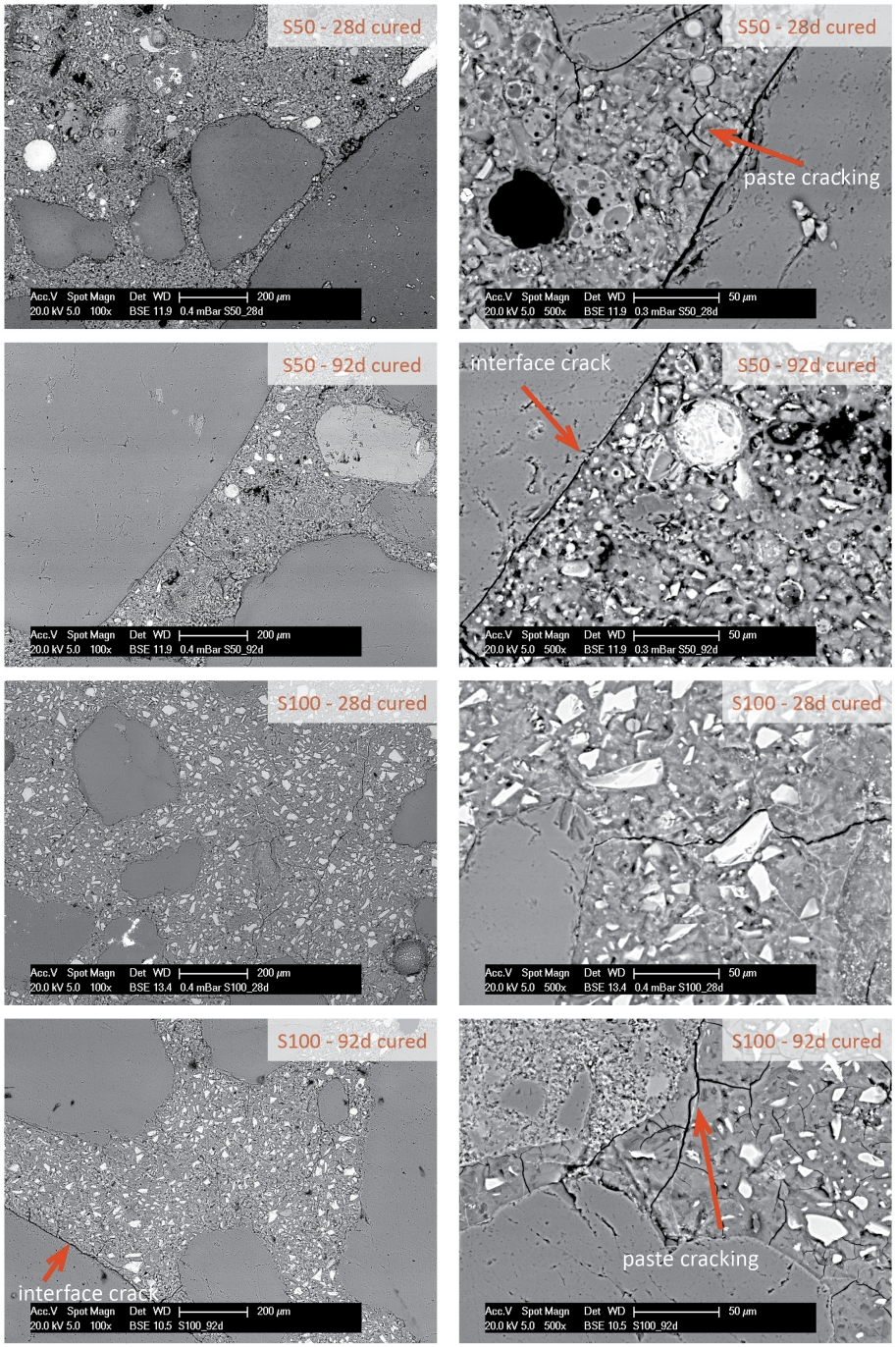


**FIGURE 14** ESEM images for S100 (100% slag) and S50 (50% slag and 50% fly ash) concrete. The two columns have different magnification factors

- This research has confirmed that AAC containing BFS can show a decrease of strength and stiffness properties over time, at least for the investigated mixtures and chosen curing conditions, implying that samples at the age of 28 days are taken out from the moist room (95%RH and 20°C) and exposed to laboratory conditions (50% RH and 20°C) until the age of testing (up to around 2 years). This, however, does not imply that every AAC mixture, or different curing conditions would show the same behavior.
- The obtained results show a decrease of mechanical properties (elastic modulus, tensile splitting strength and flexural strength) over time, for both investigated mixtures cured for 28 days in the moist room curing conditions. Especially for elastic modulus, quite a significant decrease of around 35% between 28 and 695 days has been observed for mix S50. 89% of this decrease took part until the age of 91 days. For mix S100, after the age of 91 days, the tensile splitting strength shows the trend of increase, but at the age of 695 days it is still lower compared to 28 days value.
- The acquired results from the experiments show that S50 is characterized by a higher degree of decrease over time

than S100 for tensile splitting strength, flexural strength and elastic modulus. Based on these results, it is not very likely that the decrease is directly related to the amount of BFS in the binder.

- The acquired results indicate that the observed decrease of properties, also reported for regular concrete, is related to drying (moisture loss). However, more research is needed to better understand the observed phenomenon, especially related to the aimed practical application of AAC.
- Four-point bending tests on reinforced AAC beams showed that generally, structural behavior and development of cracks (spacing and width) seem to be comparable for reinforced AAC and conventional concrete. Furthermore, the decrease of material properties did not show to have an effect on structural behavior of reinforced AAC beams.

## ACKNOWLEDGMENTS

The authors are grateful for the research support provided by the 4TU.Bouw Lighthouse project "Towards a Geopolymer Concrete Bridge", a collaboration project between TU Delft Microlab, TU Delft Macrolab en TU Eindhoven. The assistance provided by staff from the concrete laboratory and Microlab at Delft University of Technology is truly appreciated.

## CONFLICT OF INTEREST

The authors declare no conflict of interest.

## ORCID

*Mladena Luković* https://orcid.org/0000-0002-9254-6937

## REFERENCES

1. Monteiro P, Kuhmar Mehta P. Concrete: Microstructure, properties, and materials. 3rd ed. New York, NY: McGraw-Hill Publishing, 2006.
2. Zhang Z, Provis JL, Reid A, Wang H. Geopolymer foam concrete: An emerging material for sustainable construction. Construct Build Mater. 2014;56:113–127.
3. Garcia-Lodeiro I, Palomo A, Fernández-Jiménez A. 2 - an overview of the chemistry of alkali-activated cement-based binders Handbook of Alkali-Activated Cements, Mortars and Concretes (pp. 19–47). Oxford, UK: Woodhead Publishing, 2015.
4. Provis J, van Deventer J. Alkali activated materials; state-of-the-art report, RILEM TC 224-AAM. Dordrecht, the Netherlands: Springer Netherlands, 2014.
5. Collins FG, Sanjayan JG. Microcracking and strength development of alkali activated slag concrete. Cement Concrete Compos. 2001;23(4–5):345–352.
6. Wardhono A, Gunasekara C, Law DW, Setunge S. Comparison of long term performance between alkali activated slag and fly ash geopolymer concretes. Construct Build Mater. 2017;143:272–279.
7. Prinsse S (2017), Alkali-activated concrete: Development of material properties (strength and stiffness) and flexural behaviour of reinforced beams over time [Master Thesis]. Delft: Delft University of Technology.
8. Nedeljković M. Carbonation mechanism of alkali-activated fly ash and slag materials: In view of long-term performance predictions. PhD thesis. The Netherlands: Delft University of Technology, 2019;p. 2019.
9. Aldin Z, Nedeljković M, Luković M, Liu J, Blom K, Ye G.. Optimization of a geopolymer mixture design for a reinforced cantilever concrete bench. Paper presented at the The 9th International Symposium on Cement and Concrete (ISCC 2017). 2017.
10. Arbi K, Nedeljković M, Zuo Y, Ye G. Durability of alkali-activated fly ash and slag concrete. Paper presented at the The 9th International Concrete Conference 2016-Environment, Efficiency and Economic Challenges for Concrete (Dundee, Scotland); 2016.
11. Arbi K, Nedeljković M, Zuo Y, Grünewald S, Keulen A, Ye G.. Experimental study on workability of alkali activated fly ash and slag-based geopolymer concretes. Paper presented at the Geopolymers 2015 – An ECI Conference, Austria; 2015.
12. Nedeljković M, Zuo Y, Arbi K, Ye G. Natural carbonation of alkali-activated fly ash and slag pastes. In Hordijk DA, Luković M, editors. High tech concrete: Where technology and engineering meet: Proceedings of the 2017 fib Symposium, held in Maastricht, The Netherlands: Springer International Publishing, June 12–14, 2017. p. 2213–2223.
13. Corr D, Accardi M, Graham-Brady L, Shah S. Digital image correlation analysis of interfacial debonding properties and fracture behavior in concrete. Eng Fract Mechan. 2007;74(1):109–121.
14. Eberl C, Thompson R, Gianola D. Digital image correlation and tracking with Matlab. Matlab Central File Exchange; 2006.
15. Shah S, Kishen JC. Fracture properties of concrete–concrete interfaces using digital image correlation. Exp Mech. 2011;51(3):303–313.
16. Lee NK, Lee HK. Setting and mechanical properties of alkali-activated fly ash/slag concrete manufactured at room temperature. Construct Build Mater. 2013;47(15):1201–1209.
17. Thomas RJ, Peethamparan S. Alkali-activated concrete: Engineering properties and stress–strain behavior. Construct Build Mater. 2015;93:49–56.
18. Huang Z. Flexural behaviour of reinforced concrete beams with a layer of SHCC in the tension zone - Experimental Study [master thesis], Delft University of Technology, Delft; 2017.
19. Shah A, Shah CB. Comparison of load-displacement relationship and crack development mechanism in reinforced geopolymer concrete beams with that of regular reinforced concrete Beams. Paper presented at the RILEM 2017, Chennai, India; 2017.
20. Kumaravel S, Thirugnanasambandam S. Flexural behaviour of geopolymer concrete beams. India: Annamalai University, 2013.
21. Mors RM. Autogenous shrinkage of cementitious materials containing BFS [Master Thesis], Delft University of Technology, Delft; 2011.
22. Maruyama I, Sasano H, Nishioka Y, Igarashi G. Strength and Young's modulus change in concrete due to long-term drying and heating up to 90°C. Cem Concr Res. 2014;66:48–63.

## AUTHOR BIOGRAPHIES

Silke Prinsse, graduated MSc student
Delft University of Technology
Delfts, the Netherlands
silkeprinsse@outlook.com

Dick Arend Hordijk, Professor
Delft University of Technology
Delfts, the Netherlands
hordijk@adviesbureau-hageman.nl

Guang Ye, Associate Professor
Delft University of Technology
Delfts, the Netherlands
g.ye@tudelft.nl

Paul Lagendijk, Lecturer
Delft University of Technology
Delfts, the Netherlands
ir.paul.lagendijk@gmail.com

Mladena Luković, Assistant Professor
Delft University of Technology
Delfts, the Netherlands
m.lukovic@tudelft.nl

**How to cite this article:** Prinsse S, Hordijk DA, Ye G, Lagendijk P, Luković M. Time-dependent material properties and reinforced beams behavior of two alkali-activated types of concrete. *Structural Concrete*. 2020;21:642–658. https://doi.org/10.1002/suco.201900235